ECCOMAS Congress 2016
VII European Congress on Computational Methods in Applied Sciences and Engineering
M. Papadrakakis, V. Papadopoulos, G. Stefanou, V. Plevris (eds.)
Crete Island, Greece, 5–10 June 2016

FLOW FIELD ESTIMATION IN OPEN CHANNEL BASED ON KALMAN FILTER FINITE ELEMENT METHOD

T. Yoshiara[1], T. Kurahashi[2], Y. Kobayashi[3], and T. Eto[4]

[1] Graduate school of Nagaoka University of Technology,
1603-1 Kamitomioka, Nagaoka, Niigata, 940-2188, Japan.
e-mail: s133085@stn.nagaokaut.ac.jp

[2] Department of Mechanical Engineering, Nagaoka University of Technology,
1603-1 Kamitomioka, Nagaoka, Niigata, 940-2188, Japan.
e-mail: kurahashi@mech.nagaokaut.ac.jp

[3] Department of Mechanical Engineering, Nagaoka University of Technology,
1603-1 Kamitomioka, Nagaoka, Niigata, 940-2188, Japan.
e-mail: kobayasi@mech.nagaokaut.ac.jp

[4] National Institute of Technology Nagaoka college,
888 Nishikatakai, Nagaoka, Niigata, 940-8532, Japan.
e-mail: eto@nagaoka-ct.ac.jp

Keywords: Finite element method, Kalman filter theory, Estimation of flow field

Abstract. *The Kalman filter developed by R. E. Kalman and R. S. Bucy is states estimation theory in the target domain and has been employed in various field of engineering. In general, observation data in any system include observation noise and the computational model includes system noise. The finite element equation is applied to derive the state transition matrix in the system equation of the Kalman filter. We can estimate state values after the time progress of spatial models. On the other hand, tidal power generation has the potential to contribute significantly as one of the clean energy. In tidal power generation, propellers of generator are rotated by tidal current and tidal power is converted to electric energy. Therefore, the generator should be placed in the fast point of tidal current to produce more electric energy. Thus, we focused on the flow field estimation using the observation data at limited observation points to find out the fast point of tidal current. As the fundamental study, the estimation of the flow field in open channel is carried out based on the finite element method and the Kalman filter theory. As the governing equation, the shallow water equations are employed, and the finite element and the selective lumping methods are applied to discretize the governing equations in space and time, respectively. The estimation of the distribution of the velocity vector and the water elevation is carried out by using the discretized equation. The open channel model is employed in the numerical experiment, and some examinations are carried out by changing the observation variables, number and position of observation points. In addition, numerical experiments using practical observed values are carried out.*

1 INTRODUCTION

In this study, the estimation of the flow field is carried out based on the finite element method and the Kalman filter theory in open channel. Figure 1 shows an example of open channel. As the governing equation, the shallow water equation is employed, and the finite element and the selective lumping methods are applied to discretize the governing equation in space and time, respectively. The estimation of the distribution of the velocity vector and the water elevation is carried out by using the discretized equation obtained by the Kalman filter theory. In the numerical experiments, the open channel flow is treated, and some examinations are carried out by changing the observation variables, number and position of observation points.

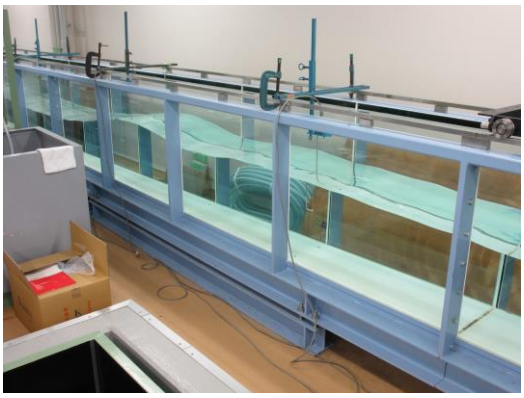

Figure 1: Open channel.

2 DISCRETIZATION OF GOVERNING EQUATIONS

The shallow water equations are used as a governing equations, which is represented as equation (1) and (2) in the two-dimensional plane.

$$\dot{u}_i + g\eta_{,i} = 0 \tag{1}$$

$$\dot{\eta} + hu_{,i} = 0 \tag{2}$$

where u, η, g, and h are flow velocity, water elevation, the gravitational acceleration and water depth. The Galerkin method and the selective lumping method are applied to discretize the governing equations in space and time, respectively. Consequently, the finite element equation can be written as equation (3). Equation (3) is represented by equation (4).

$$\begin{Bmatrix} \{u^{n+1}\} \\ \{v^{n+1}\} \\ \{\eta^{n+1}\} \end{Bmatrix} = \begin{bmatrix} [\overline{M}] & [0] & [0] \\ [0] & [\overline{M}] & [0] \\ [0] & [0] & [\overline{M}] \end{bmatrix}^{-1} \begin{bmatrix} [\tilde{M}] & [0] & -g\Delta t[S_x] \\ [0] & [\tilde{M}] & -g\Delta t[S_y] \\ -\overline{h}\Delta t[S_x] & -\overline{h}\Delta t[S_y] & [\tilde{M}] \end{bmatrix} \begin{Bmatrix} \{u^n\} \\ \{v^n\} \\ \{\eta^n\} \end{Bmatrix} \tag{3}$$

$$\{\hat{\phi}^{n+1}\} = [A]\{\hat{\phi}^n\} \tag{4}$$

where, Δt, $\overline{h}$, $[S_i]$, $[M]$ and $[\overline{M}]$ are time increment, mean water depth in the element, the matrix for the pressure, consistent mass matrix and diagonal mass matrix. $[\tilde{M}]$ is represented as equation (5) by ramping parameter $e(0 \le e \le 1)$. $\{\hat{\phi}\}$ indicates the true value.

$$\left[\tilde{M}\right] = (1-e)\left[\overline{M}\right] + e[M] \tag{5}$$

The system equation in the Kalman filter is obtained by adding the vector represented by the multiplication of the driving matrix $[\Gamma]$ and the system noise vector $\{q\}$, and is shown as Equation (6). Here, the vector $\{\phi\}$ indicates the estimation value in computation by the Kalman filter. In addition, the observation equation shown in Equation (7) is introduced. The vectors $\{z\}$ and $\{r\}$ and the matrix $[H]$ denote the observation value and the observation noise vectors and the observation matrix.

$$\left\{\phi^{n+1}\right\} = [A]\left\{\phi^{n}\right\} + [\Gamma]\left\{q^{n}\right\} \tag{6}$$

$$\left\{z^{n+1}\right\} = [H]\left\{\phi^{n+1}\right\} + \left\{r^{n+1}\right\} \tag{7}$$

3 COMPUTATIONAL ALGORITHM

It shows the numerical calculation algorithm by Kalman filter below.

1. Set input data : $[A]$, $[P_{(+)}^{0}]$, $\{\hat{\phi}_{(+)}^{0}\}$, $[\Gamma]$, $[Q]$, $[R]$, ε, $\{z^{n+1}\}$*(n = 0~imax)*
2. Calculation of estimated error covariance matrix: $[P_{(-)}] = [A][P_{(+)}][A]^{T} + [\Gamma][Q][\Gamma]^{T}$
3. Calculation of Kalman gain matrix: $[K_1] = [P_{(-)}][H]^{T}\left([H][P_{(+)}][H]^{T} + [R]\right)^{-1}$
4. Calculation of predicted error covariance matrix: $[P_{(+)}] = [P_{(-)}] - [K_1][H][P_{(-)}]$
5. Check of convergence: if $\sqrt{tr\left(\left([P_{(+)}^{k+1}] - [P_{(+)}^{k}]\right)\left([P_{(+)}^{k+1}] - [P_{(+)}^{k}]\right)^{T}\right)} \le \varepsilon$ then go to 6, else go to 2.
6. Calculation of estimated value: $\{\hat{\phi}_{(-)}^{n+1}\} = [A]\{\hat{\phi}_{(+)}^{n}\}$
7. Calculation of optimal estimated value: $\{\hat{\phi}_{(+)}^{n+1}\} = \{\hat{\phi}_{(-)}^{n+1}\} + [K_1]\left(\{z^{n+1}\} - [H]\{\hat{\phi}_{(-)}^{n+1}\}\right)$

4 EXMINATION BY NUMERICAL EXPERIMENT

This examination is carried out by changing the observation variables, number and location of observation points. The computational conditions in this study is shown in Table 1. Computational model is shown in Figure 2.

Time increment Δt, s	0.001
Time steps	2000
Number of nodes	153
Number of elements	200
Gravitational acceleration g, m/s^2	9.8
Lumping parameter e	0.8
Initial of estimated error covariance $P_{(+)}^{0}$	1.0
Initial of estimated value $\hat{\phi}_{(+)}^{0}$	0
Convergence determination constant ε	0.01

Table 1: Computational conditions.

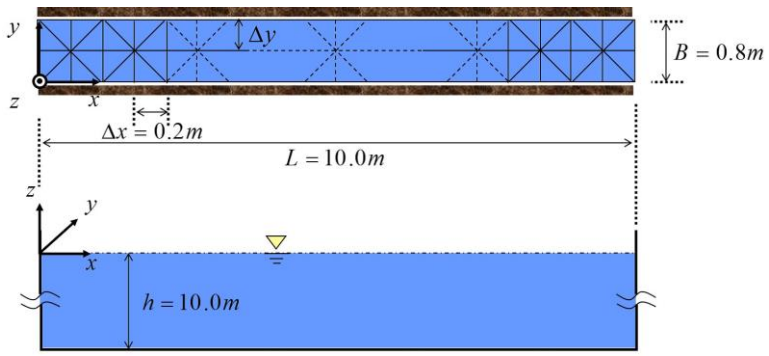

Figure 2: Computational model.

When the water elevation in amplitude 1.0m and period 2.0π s are given for the equation (5), the shallow water flow analysis is carried out. The results by this analysis are used as the artificial observation values. In this computation, the covariance for the system noise and observation noise is set 0.0001 and 0.1, respectively. The system noise covariance matrix $[Q]$ and observation noise covariance matrix $[R]$ are the diagonal matrix that diagonal component are 0.0001 and 0.100. In addition, case 'a' represents that observation variables are flow velocity for *x*-*y* direction u, v and water η and case 'b' of setting that observation variable is η only. These cases are distinguished by subscript 'a' or 'b', number of observation points and position of observation points are shown in Figure 3. Numerical results are shown in Figure 4 - 7.

	Observation variable	Position and number of observation points
Case1	Case 1a : x-y velocities and water elevation Case 1b : only water elevation	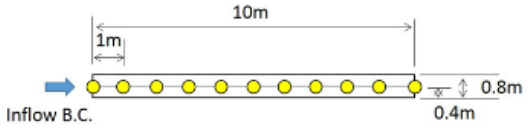
Case2	Case 2a : x-y velocities and water elevation Case 2b : only water elevation	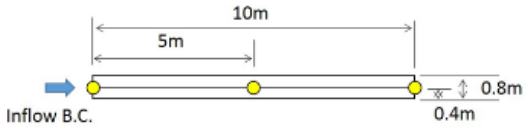
Case3	Case 3a : x-y velocities and water elevation Case 3b : only water elevation	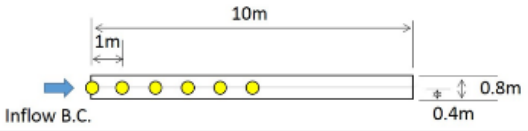
Case4	Case 4a : x-y velocities and water elevation Case 4b : only water elevation	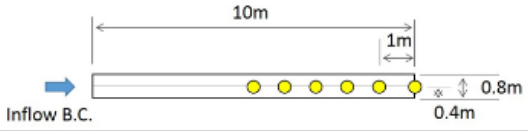
Case5	Case 5a : x-y velocities and water elevation Case 5b : only water elevation	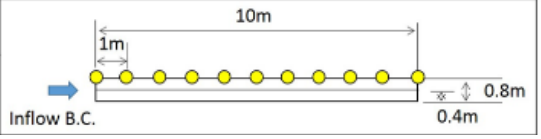

Figure 3: Numerical test conditions.

In Cases 1-4, the observation points are set on center line of the channel, and number and position of the observation points are changed. In Case 5, the observation points are set on one side of the wall boundary.

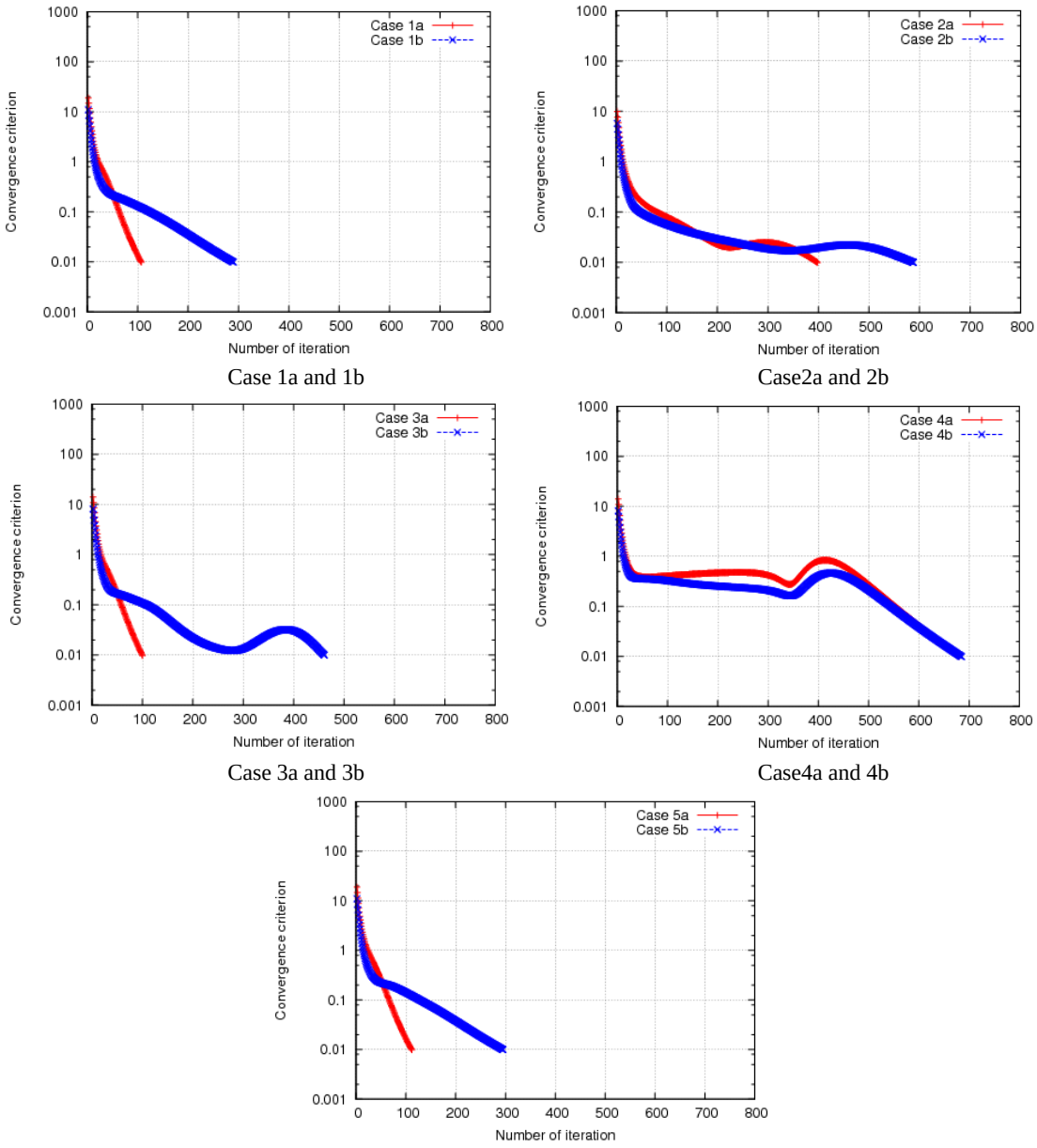

Figure 4: Comparison of variation of convergence criterion.

Figure 4 shows comparison of variation of convergence criterion expressed by the Frobenius norm. The equation of the Frobenius norm is shown in the flow chart of section 3.The convergence criterion ε is set 0.01. This convergence criterion follows to the reference by Heemink [3]. From this result, it was found that convergence rate in Case ‘a’ is faster than that in Case “b” in the iterative computation of the predicted error covariance matrix.

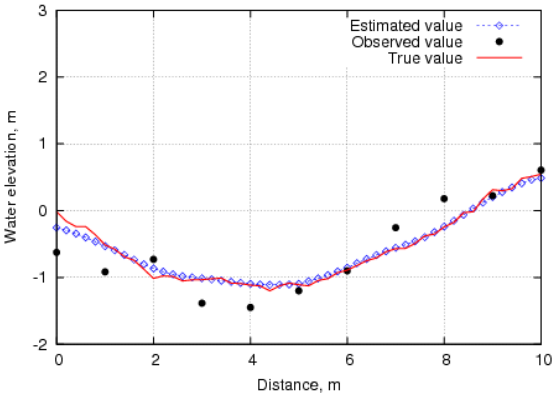

Case 1a

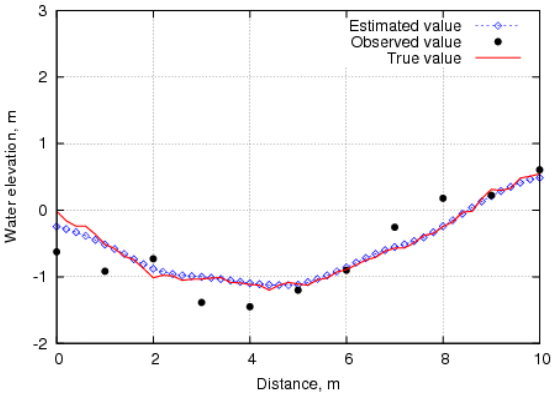

Case 1b

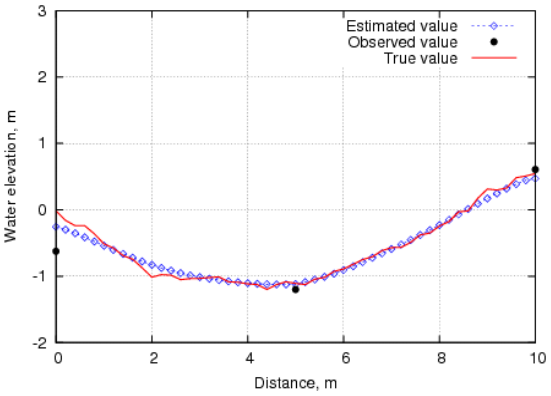

Case 2a

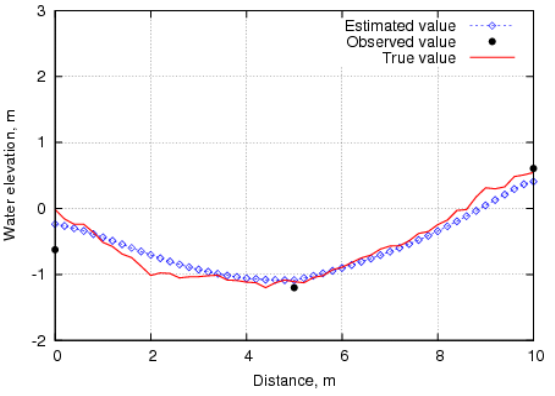

Case 2b

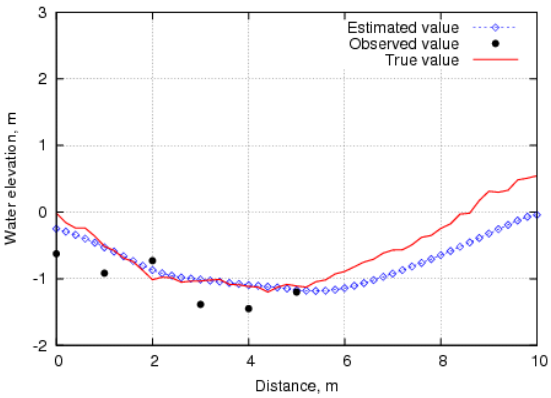

Case 3a

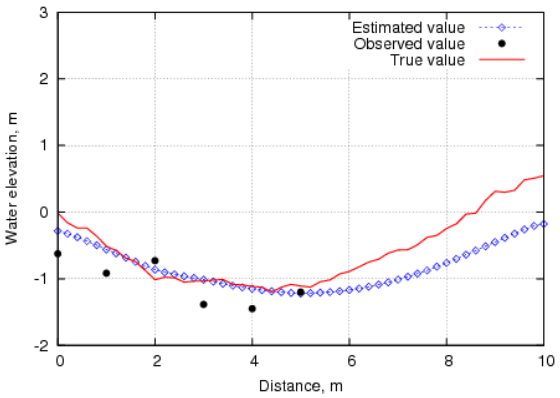

Case 3b

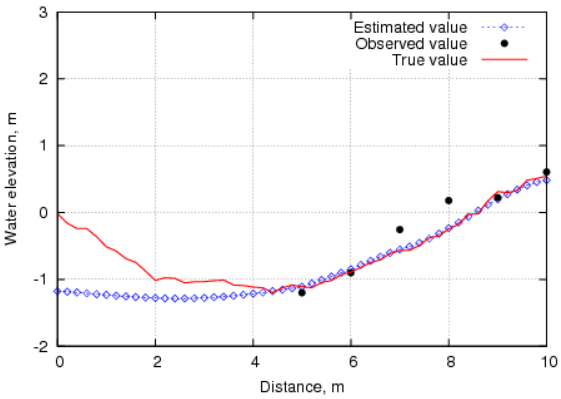

Case 4a

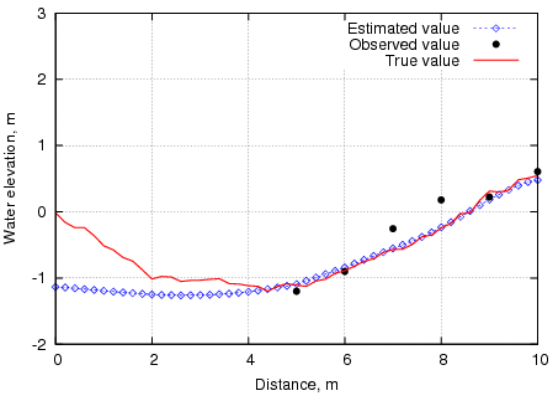

Case 4b

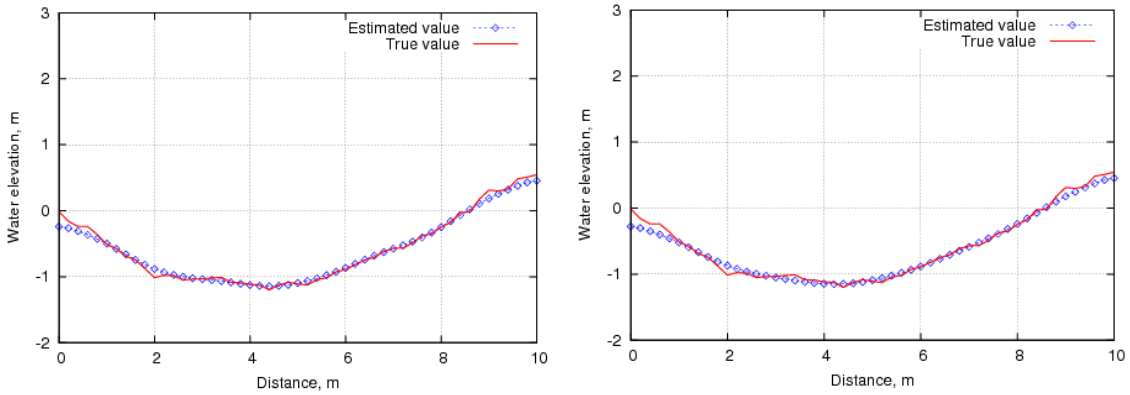

Case 5a Case 5b

Figure 5: Comparison of distribution of estimated water elevation at T =2.0s.

Figure 6 shows the distribution of estimated water elevation of the channel center line at T =2.0s. In Case 1 and Case 2, estimated values are good agreement with the true value. In Case 3, when the observation points are set on the inflow boundary side, the estimated value is good agreement with the true value in the outflow boundary side region, but, In Case 4, when the observation points are set on the outflow boundary side, it was found that it is difficult to estimate the distribution of the water elevation in inflow boundary side region. In Case 5, when the observation points are set on one side of the wall boundary, it was confirmed that the distribution of the water elevation is similar to that in Case 1.

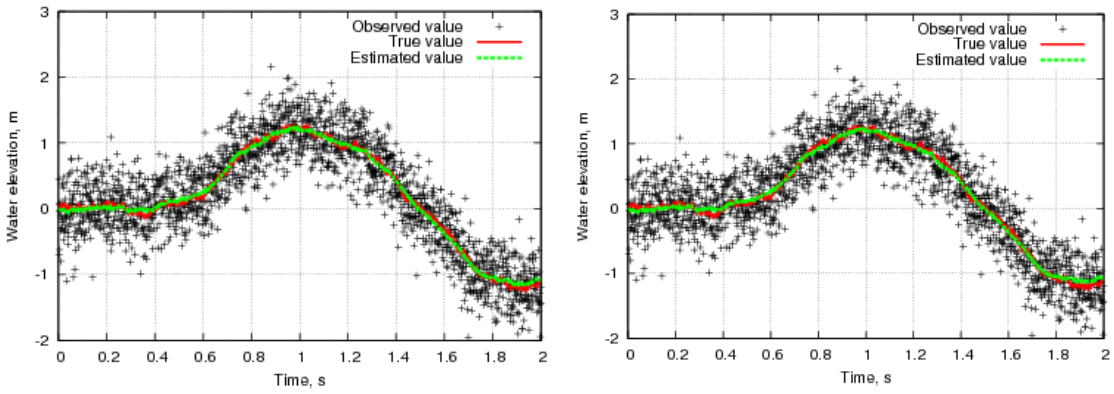

Case 1a Case 1b

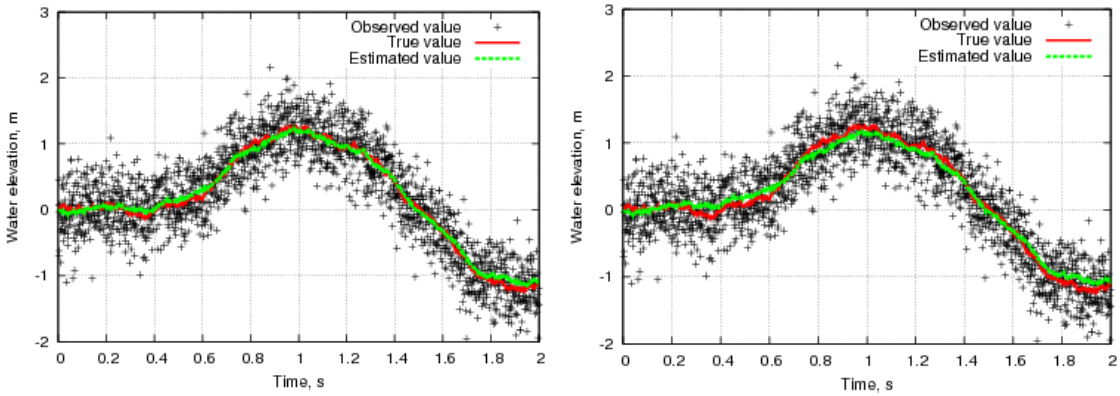

Case 2a Case 2b

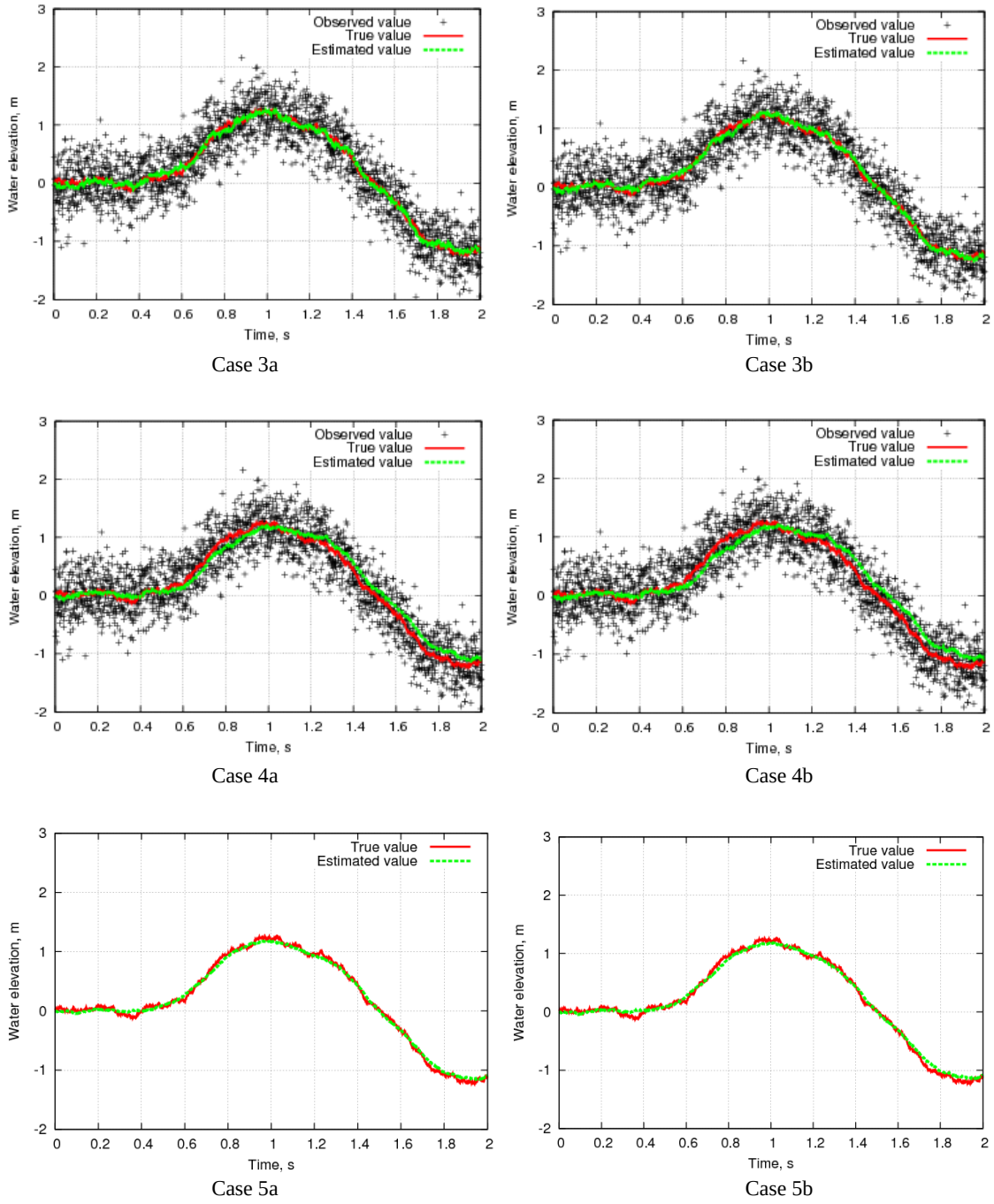

Figure 7: Comparison of time history of estimated water elevation at center point of channel (x =5.0m, y =0.4m).

Figure 7 shows time history of estimated water elevation at center point of channel (x =5.0m, y =0.4m). In all cases, observation noise is removed from observed value, and estimated values are good agreement with the true value. Table 2 shows L^2 norm for difference of true and estimated values in Figure 7. In Case 3a and Case 3b, L^2 norm is approximately equivalent. In other cases, the value of L^2 norm in Case 'a' (the flow velocity for x and y directions and the water elevation are set as the observation variable) is less than that in Case 'b' (the water elevation is only set as the observation variable.). Therefore, it can be said that estimated values in Case 'a' are better agreement with the true value than estimated values in Case 'b'.

Case	L^2 norm for difference of true and estimated values
1a	1.899
1b	1.984
2a	2.339
2b	4.050
3a	2.531
3b	2.524
4a	4.161
4b	4.988
5a	2.126
5b	2.206

Table 2: Comparison of L^2 norm for difference of true and estimated values.

5 CONCLUSIONS

In this study, flow field estimation analysis in open channel was carried out based on the Kalman filter FEM. The linear shallow water equation is employed as the governing equation, the Galarkin and the selective lumping methods are used to discretize the governing equation in space and time, respectively. The conclusions in this study is shown as follows.

- It was seen that high accurate flow field estimation result is obtained in case that the observation points are set to the downstream side in the open channel in comparison with the case that the observation points are set to the upstream side in the open channel.
- It was found that if the flow velocities for x and y directions and the water elevation are set as the observation variable in the computation of the flow field estimation, high accurate estimation result is obtained comparing to the case that the water elevation is only set as the observation variable.

APPENDIX

An example of flow field estimation using the practical measurement water elevation is shown in the appendix. The position of observation points and the size of the channel is shown in Figure 8, and the finite element mesh is shown in Figure 9. In addition, Table 3 shows the computational conditions in the flow field estimation. The flow field estimation analysis is carried out using the observed data at only points No.1 and No.2. The comparison of the time history of water elevation in case of the observed and the estimated values at points No.1 – No.3 is shown in Figures 10-12. From this result, it is found that though the flow field estimation can be carried out, there is difference between the observed and the estimated water elevation at point No.3. Therefore, it can be said that there is a possibility that flow distribution can't be appropriately obtained, if a lot of observation points are not employed, and the period of the inflow wave is short. We suppose that this is one of the future work of this study.

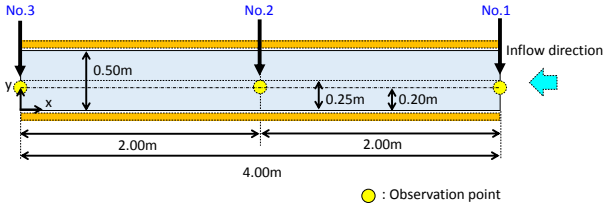

Figure 8: Size of target domain and location of observation points.

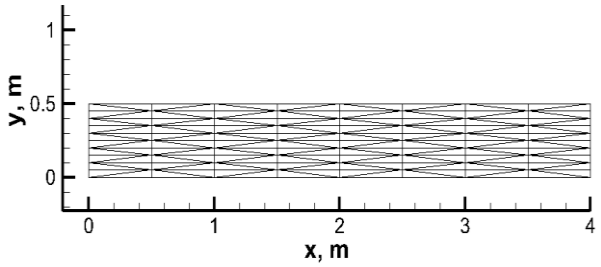

Figure 9: Finite element mesh.

Total number of nodes	99
Total number of elements	160
Time increment Δt , s	0.001
Number of time step	1000
Lumping parameter *e*	0.80
Gravitational acceleration g , m/s^2	9.8
Water depth h , m	0.46
Driving matrix $[\Gamma]$	Unit matrix
System error covariance matrix $[Q]$	$0.01\times$Unit matrix
Observation error covariance matrix $[R]$	$0.1\times$Unit matrix
Initial value of estimated error covariance matrix $[P^0_{(+)}]$	$1.0\times$Unit matrix
Initial value of state vector $\{\hat{\phi}^0_{(+)}\}$	Zero vector
Convergence criteria ε	10^{-4}

Table 3: Computational conditions.

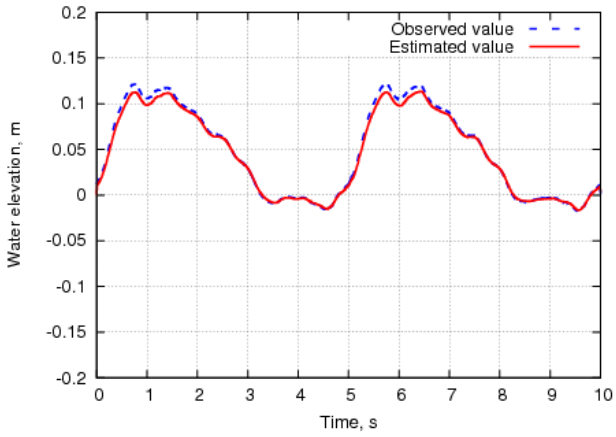

Figure 10: Comparison of water elevation at point No.1, $(x, y) = (4, 0.2)$.

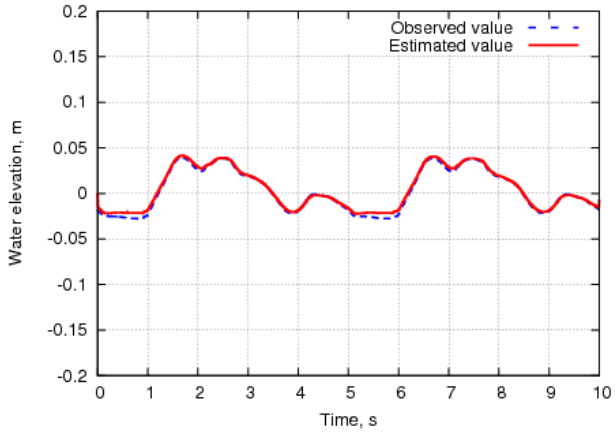

Figure 11: Comparison of water elevation at point No.2, $(x, y) = (2, 0.2)$.

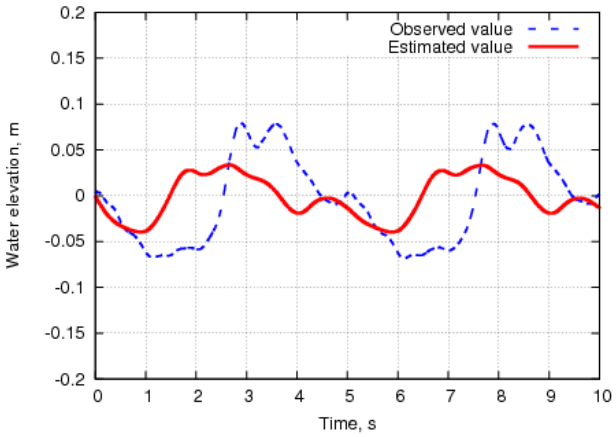

Figure 12: Comparison of water elevation at point No.3, $(x, y) = (0, 0.2)$.

ACKNOWLEDGEMENTS

This work was supported by Grants-in-Aid for scientific Research(C) Grant Number 15K05786.

REFERENCES

[1] R.E.Kalman, A New Approach to Linear Filtering and Prediction Problems, *Transactions of the ASME -Journal of Basic of Engineering*, Vol. 82， No. 1, (1960), pp.35-45.

[2] R.E.Kalman, R.S.Bucy, New Results in Linear Filtering and Prediction Theory, *Transactions of the ASME -Journal of Basic of Engineering*, Vol. 83， No. 1, (1961), pp.95-108.

[3] Heemink, A. W., Two-dimensional Shallow Water Flow Identification, Applied Mathematical Modelling, Vol. 12(1988), pp.109-118.

[4] Toshimitsu Takagi, Kosuke Inamoto, Yutaka Hayakawa, Mutsuto Kawahara, Flow estimation of shallow water by the Kalman filter finite element method, Coastal engineering proceedings， Vol. 43，(1996), pp.346-350.